Extreme waves in random crossing seas: Laboratory experiments and numerical simulations

A. Toffoli,[1] E. M. Bitner-Gregersen,[2] A. R. Osborne,[3] M. Serio,[3] J. Monbaliu,[4] and M. Onorato[3]

[1] We present an experimental and numerical investigation on the statistical properties of the surface elevation in crossing sea conditions. Experiments are performed in a very large wave basin (70 m × 50 m × 3 m) and numerical results are obtained using a higher order method for solving the Euler equations. Both experimental and numerical results indicate that the number of extreme events depends on the angle between the two interacting systems. This outcome is supported by recent theoretical investigations which have highlighted that the instability of wave packets may be triggered by the nonlinear interactions between coexisting, non-collinear wave systems. **Citation:** Toffoli, A., E. M. Bitner-Gregersen, A. R. Osborne, M. Serio, J. Monbaliu, and M. Onorato (2011), Extreme waves in random crossing seas: Laboratory experiments and numerical simulations, *Geophys. Res. Lett.*, 38, L06605, doi:10.1029/2011GL046827.

1. Introduction

[2] The research on extreme waves (also known as freak or rogue waves) in the ocean has been rapidly developing in the last ten years and has also attracted the attention of many other fields in physics. In the absence of an ambient current, one of the mechanisms which can explain the occurrence of rogue waves is the instability of a uniform narrow banded wave train to side-band perturbations (Benjamin-Feir or modulational instability, see *Zakharov and Ostrovsky* [2009] for a review). In deep water the modulational instability is described by the Nonlinear Schrödinger (NLS) equation [*Zakharov and Ostrovsky*, 2009], which is derived from the Euler equations assuming weak nonlinearity and narrow spectra.

[3] For single peaked (or unimodal) spectral conditions, the statistical properties of waves and their relation to the modulational instability have been investigated in a number of theoretical [*Janssen*, 2003], experimental [*Onorato et al.*, 2009; *Waseda et al.*, 2009] and numerical studies [*Onorato et al.*, 2001; *Socquet-Juglard et al.*, 2005; *Chalikov*, 2009]. Findings have revealed that the instability of wave packets is indeed responsible for a substantial increase of the probability of occurrence of extreme waves which yields to strong deviations from Gaussian statistics (Normality), provided

the wave spectrum is sufficiently steep and narrow banded both in the frequency and directional domain.

[4] Very often, however, ocean wave spectra are characterized by the coexistence of two wave systems with different directions of propagation. This condition, which is known as a crossing sea, implies that the energy is concentrated over two different spectral peaks (i.e., bimodal spectrum). In the present Letter, we discuss the occurrence of extreme waves and deviations from Normality in crossing sea conditions. In particular, we intend to show that the deviation from Gaussian statistics depends on the angle between the two wave systems.

[5] From a theoretical point of view, the stability of a system of two non-collinear wave trains can be described to the leading order in dispersion and nonlinearity by the following set of coupled NLS equations [see *Roskes*, 1976; *Onorato et al.*, 2006; *Shukla et al.*, 2006]:

$$\frac{\partial A}{\partial t} - i\alpha \frac{\partial^2 A}{\partial x^2} + i\left(\xi|A|^2 + 2\zeta|B|^2\right)A = 0 \qquad (1)$$

$$\frac{\partial B}{\partial t} - i\alpha \frac{\partial^2 B}{\partial x^2} + i\left(\xi|B|^2 + 2\zeta|A|^2\right)B = 0 \qquad (2)$$

The analytical forms of the coefficients in (1) and (2) are reported by *Onorato et al.* [2006]. To the leading order in nonlinearity, the surface elevation $\eta(x, y, t)$ is related to the envelopes A and B in the following way:

$$\eta = \frac{1}{2}\left(Ae^{i(kx+ly-\omega t)} + Be^{i(kx-ly-\omega t)}\right) + c.c. \qquad (3)$$

where c.c. stands for complex conjugate; (k, l) and $(k, -l)$ are the coordinate in Fourier space of the two carrier waves; $\omega = \sqrt{g\kappa}$, with $\kappa = \sqrt{k^2 + l^2}$ and g is gravity acceleration. The angle between the two wave systems is defined as $\beta = 2\arctan(l/k)$. A linear stability analysis of plane wave solutions of (1) and (2) [*Ioualalen and Kharif*, 1994; *Badulin et al.*, 1995; *Onorato et al.*, 2006; *Shukla et al.*, 2006] indicates that not only do the growth rates of perturbations moving along the main direction of propagation depend on the length of the perturbation but also on the angle between the two wave systems. In this respect, growth rates different from zero are found for $0 < \beta < \arctan(\sqrt{2}/2) \simeq 70.53°$. As β approaches $\beta_c \approx 70.53°$, the nonlinear terms in the coupled system become increasingly more important. Consequently, the ratio between nonlinearity and dispersion, a measure for the presence of extreme waves in single NLS [*Onorato et al.*, 2001; *Janssen*, 2003], increases substantially (see *Onorato et al.* [2010, Figure 2] for details). For $\beta > \beta_c$, however, the ratio changes sign and the coupled NLS

---

[1]Faculty of Engineering and Industrial Sciences, Swinburne University of Technology, Hawthorn, Victoria, Australia.
[2]Det Norske Veritas A.S., Høvik, Norway.
[3]Dipartimento di Fisica Generale, Universitá di Torino, Turin, Italy.
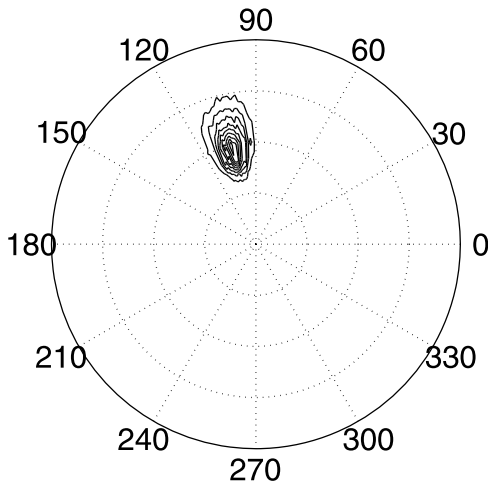[4]Department of Civil Engineering, Katholieke Universiteit Leuven, Heverlee, Belgium.

Figure 1. Derived directional spectrum [*Donelan et al.*, 1996] near the absorbing beach opposite the wave-maker for a wave system propagating towards the vertical wall. Circles indicate frequency (from 0.5 *Hz*, inner circle, to 2 *Hz*, outer circle), while straight lines indicate directions (°); 90° is the direction normal to the wave-maker.

change from focusing to defocusing. For random waves, we can expect that larger deviations from Normality already begin for $\beta > 40°$ [*Onorato et al.*, 2010]. Interestingly enough, the growth rate decreases and eventually becomes zero for β approaching β_c. Hence, deviations from Normality should decrease for angle β close to 70.53°.

[6] In order to verify this conjecture, here we present a unique laboratory experiment, which was designed to observe the nonlinear dynamics of non-collinear, co-propagating, random wave trains. A qualitative description of the role of modulational instability in crossing seas is then provided by numerical simulations of a third order truncation of the potential Euler equations [*West et al.*, 1987]. The fourth order moment of the surface elevation (kurtosis), which is strictly related to the probability of appearance of a freak waves [see *Janssen*, 2003], is here discussed as a function of the angle between the wave systems.

2. Laboratory Experiments

[7] Laboratory tests were performed in the directional wave tank at Marintek (Norway). The facility has dimensions of 70 *m* × 50 *m* and is fitted with a directional wave-maker along the 70 *m* side. The tank is also equipped with two minimum-reflection beaches: one is located in front of the directional wave-maker, while a second one is on the right-hand 50-*m* side. For the present experiments the water depth was fixed at 3 *m*.

[8] Irregular waves were mechanically generated according to an input directional spectrum $E(\omega, \vartheta)$, where ω is the angular frequency and ϑ is the direction. Amplitudes were randomly chosen from the Rayleigh distribution, while the random phases were assumed to be uniformly distributed in the interval $[0, 2\pi]$. The input spectrum was composed by the sum of two identical JONSWAP spectra [*Komen et al.*, 1994] describing two long-crested wave fields, propagating along two different directions. Each spectrum has a peak period $T_p = 1$ *s*, which corresponds to a peak wave length

$\lambda_p = 1.56$ *m*, a significant wave height $H_s = 0.068$ *m* and a peak enhancement factor $\gamma = 6$; the wave steepness is $k_p a = 0.14$, where k_p is the wavenumber at the spectral peak and $a = H_s/2$. The systems were forced to propagate along two different directions, which are symmetrical with respect to the normal to the wave-maker. The following angles between the two systems were considered: $\beta = 10°$, 20°, 30° and 40°. Note that for random wave fields the perturbations can propagate along the main direction of propagation as well as the incident direction of each system. The latter, may trigger a type of instability (instability of type Ib [*Ioualalen and Kharif*, 1994]), which differs from the conditions imposed in (1) and (2), where the perturbation only moves along the main direction of propagation.

[9] Throughout the experiments, the surface elevation was measured at a sampling frequency of 80 *Hz*. Probes were deployed along the main axis of the basin every 5 meters (see *Onorato et al.* [2009] for details). In order to have enough samples to produce a statistical analysis, four realizations of the random sea surface with the same imposed spectrum were performed with different sets of random amplitudes and phases. For each test, 20-minute time series were collected, including the initial ramp-up; about 4500 individual waves were measured at every probes.

[10] Note that, whereas the wave system moving rightward is completely absorbed by the beaches, waves moving leftward are inevitably reflected by the side wall. Preliminary tests using monochromatic waves with leftward propagation and period and amplitude consistent with T_p and H_s did not reveal the presence of any reflection for directions $\beta/2 \leq 20°$ with respect to the normal to the wave-maker. To further dispel any doubts, a few tests were also repeated with unimodal irregular wave fields. An observed energy spectrum at about 22.5 peak wavelengths from the wave-maker (nearby the beach) is presented in Figure 1; directional properties were derived by using the wavelet directional method [*Donelan et al.*, 1996]. This measurement shows that the energy remained confined within a range of leftward directions, thus excluding the presence of reflected waves.

3. Numerical Simulations

[11] To support the experimental results qualitatively, direct numerical simulations of the potential Euler equations with initial conditions nominally identical to the ones applied in tank were performed. Assuming the hypothesis of an irrotational, inviscid and incompressible fluid flow, the velocity potential $\phi(x, y, z, t)$ satisfies the Laplace's equation everywhere in the fluid. At the bottom, $z = -\infty$, the vertical velocity is zero; at the free surface, $z = \eta(x, y, t)$, the following kinematic and dynamic boundary conditions hold [see *Zakharov and Ostrovsky*, 2009]:

$$\psi_t + g\eta + \frac{1}{2}\left(\psi_x^2 + \psi_y^2\right) - \frac{1}{2}W^2\left(1 + \eta_x^2 + \eta_y^2\right) = 0, \quad (4)$$

$$\eta_t + \psi_x\eta_x + \psi_y\eta_y - W\left(1 + \eta_x^2 + \eta_y^2\right) = 0, \quad (5)$$

where $W(x, y, t) = \phi_z|_\eta$ is the vertical velocity at the free surface and $\psi(x, y, t)$ is the potential calculated at the surface. Numerical simulations of (4) and (5) were performed
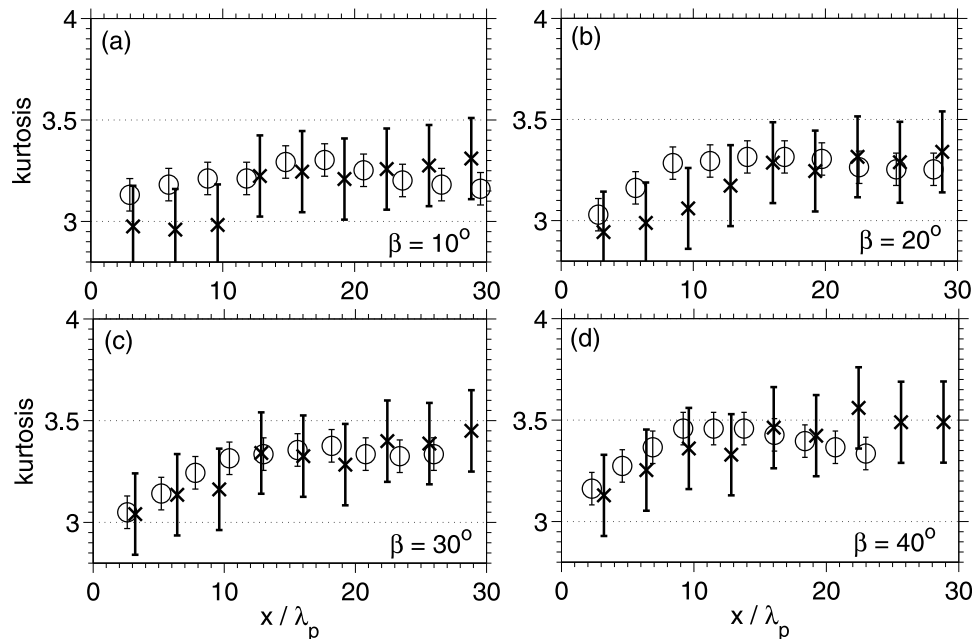
Figure 2. Evolution of kurtosis along the tank (x refers to the distance from the wave-maker): laboratory experiments (crosses); numerical simulations (circles).

with the Higher Order Spectral Method (HOSM) proposed by *West et al.* [1987] under the assumption of weak non-linearity. This is a pseudo-spectral method that uses a series expansion in the wave slope of $W(x, y, t)$ about the free surface to estimate the surface elevation and velocity potential at each time step. Here a third order expansion is used so that modulational instability can be modeled. This approach provides a good approximation of the evolution of three-dimensional, mechanically generated random waves with a unimodal spectral distribution [*Toffoli et al.*, 2010]. Note, however, that other methods can be employed to simulate crossing wave fields [see, e.g., *Ruban*, 2009].

[12] The initial surface elevation was calculated from the input spectrum by first switching from (ω, ϑ) to (k_x, k_y) coordinates and then using an inverse Fourier transform with the random amplitude and phase approximation. The velocity potential $\psi(x, y, t = 0)$ was obtained from the input surface with linear theory. The wave field was contained in a square domain of about 15 m with spatial mesh of 256×256 nodes; periodic boundary conditions were considered. A fourth-order Runge-Kutta method was used for the time integration. A time step of $\Delta t = T_p/100$ was employed. Aliasing errors were eliminated by truncating the spectrum for $k > 6 \ k_p$ (see, e.g., *Toffoli et al.* [2010] for further details). Numerical tests reproduced the wave evolution for a period of 60 T_p; the surface elevation and velocity potential were stored every 6 T_p. About 100 realizations with the same input spectrum and different random amplitudes and phases were performed. Numerical simulations were extended up to $\beta = 90°$ with an increasing step of 10°.

[13] Whereas the experiments provide the spatial evolution of waves along the basin, the simulations provide the temporal evolution of an initial wave field with periodic boundary conditions. This difference is a possible source of discrepancy when comparing numerics with experiments. In the following analysis the comparison is based on the

leading order approximation, i.e., space and time are related by the group velocity along the direction perpendicular to the wave-maker. Recent numerical simulations of the temporal and spatial evolution of unimodal wave fields seem to confirm the goodness of such approximation [*Toffoli et al.*, 2010]. It is important to stress that numerical simulations are only used to obtain a qualitative description of the role of modulational instability in the evolution of crossing sea states. A more accurate approximation of experimental results can be achieved with numerical wave tanks. However, a discussion on the quantitative comparison between experiments and numerical simulations is not the aim of the present letter.

4. Results

[14] An indication of the presence of extreme events in time series can be obtained by the kurtosis, i.e., the fourth order moment of the probability density function of the surface elevation. For a Gaussian random wave field, the kurtosis is equal to 3. The evolution of the kurtosis is presented in Figure 2 for both experimental and numerical data. Note that the kurtosis requires very large data sets to minimize the statistical uncertainty. To quantify the latter, the 95% confidence intervals are shown in Figure 2; these intervals are calculated with bootstrap methods [*Emery and Thomson*, 2001]. Due to the limited number of waves measured in the tank, experiments are subjected to a rather large error band of about ±0.2. Numerical simulations, on the other hand, are more accurate due to the large number of realizations: the confidence interval is approximately ±0.08.

[15] Laboratory observations reveal that the kurtosis increases almost monotonically as waves propagate along the tank. Qualitatively, this growth is generally recovered by the numerical simulations during the first 15–20 wavelengths, while a decreasing trend is observed thereafter. Note that there are some quantitative discrepancies between
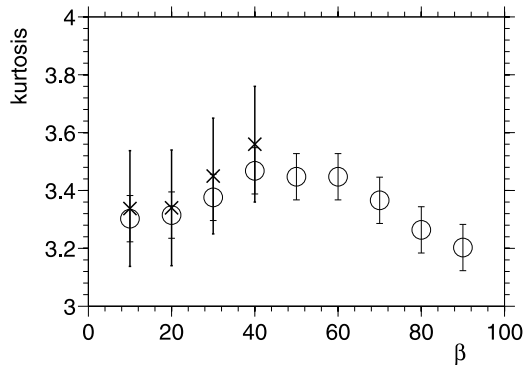
Figure 3. Maximum recorded kurtosis as a function of β: laboratory experiments (crosses); numerical simulations (circles).

experimental and numerical results. These differences, however, are confined within the concurrent confidence intervals and may not be statistically significant. We should recall, nonetheless, that the experimental and numerical set-up are not exactly the same. Because we cannot be sure *a priori* that the wave-maker is capable to properly reproduce bimodal conditions, the actual wave spectrum in the tank may differ from the initial conditions for the simulations. Furthermore, the kurtosis in the wave tank is then measured from time series at different distances from the wave-maker, while the kurtosis is calculated at fixed time from a surface in the numerical computations. The kurtosis as a function of space from numerical simulations is then converted into kurtosis as a function of time using the group velocity normal to the wave-maker. Note also that in random sea states the perturbations can propagate along both the main direction of propagation (normal to the wave-maker) and the mean direction of the incident wave systems. The latter could not be properly modeled numerically due to the limited dimension of the physical domain. All these limitations can contribute to the observed discrepancy. Despite these differences, however, laboratory and numerical tests qualitatively show that there is a consistent tendency for the kurtosis to increase with the increase of β. This is highlighted in Figure 3, where the maximum recorded kurtosis is displayed as a function of the angle β. It is important to remark that the differences between experimental and numerical records are well within the confidence intervals and hence can be attributed to statistical uncertainty. For $\beta > 40°$, experimental results are not available due to the limitation of that wave-maker to generate waves at large angles. Fortunately, numerical computations for large angles do not present any limitations. In this respect, simulations show that the kurtosis remains more or less constant from $40°$ to $60°$ and then starts decreasing. The observed dependency of the kurtosis from the angle β is consistent with the qualitative predictions based on the analysis of the coupled NLS equations.

5. Conclusions

[16] Laboratory experiments and numerical simulations of a third order truncation of the potential Euler equations were carried out to investigate the statistical properties of crossing sea states. A simple prediction based on the coupled NLS

equations was also reported. A number of angles between two identical, non-collinear systems were investigated. Results showed that the kurtosis, a measure of the probability of occurrence of extreme waves, depends on the angle between the crossing systems. Numerical simulations furthermore suggest that the maximum value is achieved for $40° < \beta < 60°$. Note that although the presented analysis is affected by the limitations of the laboratory experiment and assumptions adopted in numerical models the results show qualitatively the identical trend. It is important to mention that crossing seas can be far more complicated than the ones investigated here. Therefore, research is still called for to fully understand the role of the interaction between co-propagating wave trains for the occurrence of extreme waves.

References

Badulin, S. I., V. I. Shrira, C. Kharif, and M. Ioualalen (1995), On two approaches to the problem of instability of short-crested water waves, *J. Fluid Mech.*, *303*, 297–326.
Chalikov, D. (2009), Freak waves: Their occurrence and probability, *Phys. Fluids*, *21*, 076602, doi:10.1063/1.3175713.
Donelan, M. A., W. M. Drennan, and A. K. Magnusson (1996), Non-stationary analysis of the directional properties of propagating waves, *J. Phys. Oceanogr.*, *26*, 1901–1914.
Emery, W., and R. Thomson (2001), *Data Analysis Methods in Physical Oceanography*, Adv. Ser. Ocean Eng., vol. 2, 638 pp., Elsevier Sci., Amsterdam.
Ioualalen, M., and C. Kharif (1994), On the subharmonic instabilities of steadies three-dimensional deep water waves, *J. Fluid Mech.*, *262*, 265–291.
Janssen, P. A. E. M. (2003), Nonlinear four-wave interaction and freak waves, *J. Phys. Oceanogr.*, *33*, 863–884.
Komen, G., L. Cavaleri, M. Donelan, K. Hasselmann, H. Hasselmann, and P. Janssen (1994), *Dynamics and Modeling of Ocean Waves*, Cambridge Univ. Press, Cambridge, U. K.
Onorato, M., A. R. Osborne, M. Serio, and S. Bertone (2001), Freak waves in random oceanic sea states, *Phys. Rev. Lett.*, *86*, 5831–5834.
Onorato, M., A. Osborne, and M. Serio (2006), Modulational instability in crossing sea states: A possible mechanism for the formation of freak waves, *Phys. Rev. Lett.*, *96*, 14503, doi:10.1103/PhysRevLett.96.014503.
Onorato, M., et al. (2009), Statistical properties of mechanically generated surface gravity waves: A laboratory experiment in a 3D wave basin, *J. Fluid Mech.*, *627*, 235–257.
Onorato, M., D. Proment, and A. Toffoli (2010), Freak waves in crossing seas, *Eur. Phys. J. Spec. Top.*, *185*, 45–55, doi:10.1140/epjst/e2010-01237-8.
Roskes, G. J. (1976), Nonlinear multiphase deep-water wavetrains, *Phys. Fluids*, *19*, 1253–1254, doi:10.1063/1.861609.
Ruban, V. (2009), Two different kinds of rogue waves in weakly crossing sea states, *Phys. Rev. E*, *79*, 65304, doi:10.1103/PhysRevE.79.065304.
Shukla, P., I. Kourakis, B. Eliasson, M. Marklund, and L. Stenflo (2006), Instability and evolution of nonlinearly interacting water waves, *Phys. Rev. Lett.*, *97*, 94501, doi:10.1103/PhysRevLett.97.094501.
Socquet-Juglard, H., K. Dysthe, K. Trulsen, H. Krogstad, and J. Liu (2005), Distribution of surface gravity waves during spectral changes, *J. Fluid Mech.*, *542*, 195–216.
Toffoli, A., O. Gramstad, K. Trulsen, J. Monbaliu, E. M. Bitner-Gregersen, and M. Onorato (2010), Evolution of weakly nonlinear random directional waves: Laboratory experiments and numerical simulations, *J. Fluid Mech.*, *664*, 313–336, doi:10.1017/S002211201000385X.

Waseda, T., T. Kinoshita, and H. Tamura (2009), Evolution of a random directional wave and freak wave occurrence, *J. Phys. Oceanogr.*, *39*, 621–639.

West, B. J., K. A. Brueckner, R. S. Jand, D. M. Milder, and R. L. Milton (1987), A new method for surface hydrodynamics, *J. Geophys. Res.*, *92*, 11,803–11,824.

Zakharov, V., and L. Ostrovsky (2009), Modulation instability: The beginning, *Physica D*, *238*, 540–548.

E. M. Bitner-Gregersen, Det Norske Veritas A.S., N-1322 Høvik, Norway.

J. Monbaliu, Department of Civil Engineering, Katholieke Universiteit Leuven, B-3001 Heverlee, Belgium.

M. Onorato, A. R. Osborne, and M. Serio, Dipartimento di Fisica Generale, Universitá di Torino, I-10125 Torino, Italy.

A. Toffoli, Faculty of Engineering and Industrial Sciences, Swinburne University of Technology, Hawthorn, Vic 3122, Australia. (toffoli.alessandro@gmail.com)